Critical structure factor in Ising systems

Victor Martín-Mayor,[1,2,*] Andrea Pelissetto,[1,†] and Ettore Vicari[3,‡]
[1]*Dipartimento di Fisica dell'Università di Roma La Sapienza and INFN, I-00185 Roma, Italy*
[2]*Statistical Mechanics Center (SMC), INFM, I-00185 Roma, Italy*
[3]*Dipartimento di Fisica dell'Università di Pisa and INFN, I-56127 Pisa, Italy*
(Received 26 February 2002; published 21 August 2002)

We perform a large-scale Monte Carlo simulation of the three-dimensional Ising model on simple cubic lattices of size L^3 with $L=128$ and 256. We determine the corresponding structure factor (Fourier transform of the two-point function) and compare it with several approximations and with experimental results. We also compute the turbidity as a function of the momentum of the incoming radiation, focusing in particular on the deviations from the Ornstein-Zernike expression of Puglielli and Ford.

DOI: 10.1103/PhysRevE.66.026112 PACS number(s): 05.50.+q, 05.70.Jk, 75.10.Hk, 64.60.Fr

I. INTRODUCTION

Near a phase-transition critical point, some observed quantities show a universal behavior that is common to a large class of systems, independently of the microscopic details. A very important universality class is the Ising one, which is characterized by short-range interactions and a scalar order parameter. It describes the liquid-vapor transition in fluids, the mixing transition in multicomponent systems, and the Curie transition in (anti)ferromagnets with axial anisotropy. The Ising critical behavior has been extensively studied both theoretically and experimentally; see Refs. [1–3]. In particular, the critical exponents, the equation of state, and several amplitude ratios have been determined with good precision. Another important quantity in the theory of critical phenomena is the static structure factor, which can be measured experimentally by determining the intensity of the light scattered by the fluid relative to the intensity of the incident light [4]. To probe larger wave numbers, neutrons are used instead of light. At the critical density of fluids near the gas-liquid critical point or at the critical concentration of binary fluids near the critical mixing point, one expects for $t\equiv(T-T_c)/T_c\to 0$ the general scaling behavior [5–7]

$$S_\pm(k)=\chi g_\pm(k\xi), \tag{1}$$

where $\chi=C^\pm|t|^{-\gamma}$, ξ is the correlation length, which diverges as $\xi=f^\pm|t|^{-\nu}$, k is the momentum-transfer vector, and $\pm$ refers to the two phases $+$ $(-)$ corresponding to the high- (low-) temperature phase. Since at criticality only elastic scattering is relevant, k is given by

$$k=\frac{4\pi}{\lambda}\sin\frac{\theta}{2}, \tag{2}$$

where λ is the wavelength of the radiation (neutrons) in the scattering medium and θ is the scattering angle. The functions $g_\pm(Q)$, normalized so that

$$g_\pm^{-1}(Q)=1+Q^2+O(Q^4) \tag{3}$$

for $Q\equiv k\xi\to 0$ (this defines ξ as the second-moment correlation length), are universal. Their limiting behavior is well known. For Q small, $g_\pm(Q)$ is approximated by the leading term, the so-called Ornstein-Zernike approximation

$$g_{OZ}(Q)=\frac{1}{1+Q^2}. \tag{4}$$

Such an approximation describes well the data up to $Q\approx 1$ and is routinely used in the analysis of the data with $k\xi$ small and of the turbidity for the determination of the correlation length [8]. On the other hand, for large Q, $g_\pm(Q)$ shows an anomalous decay controlled by the exponent η:

$$g_\pm(Q)\approx\frac{C_1^\pm}{Q^{2-\eta}}. \tag{5}$$

Therefore, the experimental determination of the structure factor for large wave numbers allows a direct determination of the exponent η [9–21].

In this paper, we compute the structure factor in the high-temperature phase for small values of Q by means of Monte Carlo simulations on lattices L^3, with $L=128,256$. We are able to determine the function $g_+(Q)$ with an error of less than 1% (2%) for $Q\lesssim 5$ ($Q\lesssim 20$). These numerical results together with the most recent estimates of the critical exponents [22] are then used to determine interpolations that are valid for all values of Q and have the correct large-Q behavior. For this purpose, we use a dispersive approach [23–25], which allows us to determine an interpolating form for $g_+(Q)$ that agrees with the Monte Carlo data in the small-Q region and that well approximates (within 0.5%) the recent experimental results of Ref. [19].

These results are then used to compute the turbidity, i.e., the attenuation of the transmitted light intensity per unit optical path length due to the scattering with the sample. This

*Electronic address: Victor.Martin@roma1.infn.it
†Electronic address: Andrea.Pelissetto@roma1.infn.it
‡Electronic address: Vicari@df.unipi.it

TABLE I. Estimates of $c_n^{\pm}$, $S_M^{\pm}$, and $S_Z^{\pm}$. IHT denotes the results obtained from the analysis of high-temperature expansions for improved models, HT,LT results obtained from the analysis of high- and low-temperature expansions for the Ising model, while "ϵ-exp." and "$d=3$ g-exp." label the field-theoretical results. (sc) and (bcc) denote the simple cubic and the body-centered cubic lattice, respectively. Unless stated otherwise, field-theoretical results are taken from Ref. [30], while the IHT estimates are taken from Ref. [22]. For S_M^- we should also mention the Monte Carlo estimate of Ref. [31], $S_M^-=0.941(11)$.

	IHT	HT,LT	ϵ-exp.	$d=3$ g-exp.
c_2^+	$-3.90(6)\times10^{-4}$	$-3.0(2)\times10^{-4}$ [29] $-5.5(1.5)\times10^{-4}$ (sc) [32] $-7.1(1.5)\times10^{-4}$ (bcc) [32]	$-3.3(2)\times10^{-4}$	$-4.0(5)\times10^{-4}$
c_3^+	$0.88(1)\times10^{-5}$	$1.0(1)\times10^{-5}$ [29] $0.5(2)\times10^{-5}$ (sc) [32] $0.9(3)\times10^{-5}$ (bcc) [32]	$0.7(1)\times10^{-5}$	$1.3(3)\times10^{-5}$
c_4^+	$-0.4(1)\times10^{-6}$		$-0.3(1)\times10^{-6}$	$-0.6(2)\times10^{-6}$
S_M^+	0.999601(6)	0.99975(10) [29]	0.99968(4)	0.99959(6)
S_Z^+	1.000810(13)			
c_2^-		$-1.2(6)\times10^{-2}$ [32]	-2.4×10^{-2} [33]	
c_3^-		$7(3)\times10^{-3}$ [32]	3.9×10^{-3} [33]	
S_M^-		0.938(8) [30] 0.930(6) [34]		

quantity is routinely measured in experiments, since it allows the determination of the correlation length. In particular, we compute the deviations from the Puglielli-Ford expression [8], which is based on the Ornstein-Zernike approximation.

The paper is organized as follows. In Sec. II we review the theoretical results for the structure factor. In Sec. II A we define the basic observables and report the behavior of $g_{\pm}(Q)$ for small and large values of Q. Estimates of the constants appearing in these expansions are reported in Sec. II B. In Sec. II C we discuss Bray's approximation. First, we discuss the high-temperature phase: we update the estimates of Ref. [24] by using the most recent results for the critical exponents. Then, we generalize the approximation to the low-temperature phase. In Sec. III we discuss our high-temperature Monte Carlo results which are compared with approximate expressions and with the experimental data of Refs. [10,19]. In Sec. IV we compute the turbidity, focusing on the deviations from the Puglielli-Ford expression [8] due to the anomalous decay of $g_+(Q)$. We find that the turbidity is larger than this expression by 1% (5%) for $Q_0=15$ (350), where $Q_0=q_0\xi$ and q_0 is the momentum of the incoming radiation.

II. THEORETICAL RESULTS

A. Definitions

Several theoretical results are available for the structure factor. For Q small, one can compute the corrections to the Ornstein-Zernike behavior by writing

$$g_{\pm}^{-1}(Q)=1+Q^2+\sum_{n=2} c_n^{\pm} Q^{2n}. \tag{6}$$

For large Q, the structure factor behaves as

$$g_{\pm}(Q)\approx \frac{C_1^{\pm}}{Q^{2-\eta}}\left(1+\frac{C_2^{\pm}}{Q^{(1-\alpha)/\nu}}+\frac{C_3^{\pm}}{Q^{1/\nu}}\right), \tag{7}$$

a behavior predicted theoretically by Fisher and Langer [26] and proved in the field-theoretical framework in Refs. [27,28].

Beside the constants $c_n^{\pm}$, the constants $S_M^{\pm}$ and $S_Z^{\pm}$, defined by

$$S_M^{\pm}\equiv M_{\rm gap}^2\xi^2, \tag{8}$$

$$S_Z^{\pm}\equiv \chi/(\xi^2 Z_{\rm gap}), \tag{9}$$

are of theoretical interest. Here $M_{\rm gap}$ (the mass gap of the theory) and $Z_{\rm gap}$ determine the long-distance behavior of the two-point function in x space:

$$G(x)\approx \frac{Z_{\rm gap}}{4\pi|x|}e^{-M_{\rm gap}|x|}. \tag{10}$$

The critical limits of $S_M^{\pm}$ and $S_Z^{\pm}$ are related to the imaginary zeros $\pm iQ_0$ of $g_{\pm}^{-1}(Q)$ closest to the origin by

$$S_M^{\pm}=-Q_0^2, \tag{11}$$

$$S_Z^{\pm}=\left.\frac{dg^{-1}(Q)}{dQ^2}\right|_{Q=\pm iQ_0}. \tag{12}$$

B. Numerical results

The coefficients c_n^+ turn out to be very small [7], $c_2^+ \sim 10^{-4}$, and this explains the success of the Ornstein-Zernike approximation up to $Q \sim 1$. The constants c_n^+ have been calculated by field-theoretical methods. They have been computed to $O(\epsilon^3)$ in the framework of the ϵ expansion [24] and to $O(g^4)$ in the framework of the $d=3$ fixed-dimension expansion [29]. The perturbative series have been resummed in Ref. [30] obtaining the results reported in Table I. The most precise estimates have been obtained from the analysis of their high-temperature expansions in improved models [22]; see the results labeled by IHT in Table I.

As already observed in Ref. [29], the coefficients show the pattern

$$|c_n^+| \ll |c_{n-1}^+| \ll \cdots \ll |c_2^+| \ll 1 \quad \text{for} \quad n \geqslant 3. \tag{13}$$

Therefore, a few terms of the expansion of $g_+(Q)$ in powers of Q^2 provide a good approximation of $g_+(Q)$ in a relatively large region around $Q=0$: as we shall see, deviations are less than 1% up to $Q \approx 3$. This is in agreement with the theoretical expectation that the singularity of $g_+^{-1}(Q)$ nearest to the origin is the three-particle cut [23,24]. If this is the case, the convergence radius r_+ of the Taylor expansion of $g_+^{-1}(Q)$ is $r_+ = 3\sqrt{S_M^+}$. Since (see Table I) $S_M^+ \approx 1$, at least asymptotically we should have

$$c_{n+1}^+ \approx -\frac{1}{9} c_n^+ . \tag{14}$$

This behavior can be checked explicitly in the large-N limit of the N-vector model [29].

The coefficients c_n^- are also quite small, although not as much as in the high-temperature case. Indeed, $c_2^- \approx 10^{-2}$; see Table I. They have been computed using field-theoretical methods [33] and from the analysis of low-temperature series [32]. In the low-temperature phase, one also observes the pattern (13), although the coefficients decrease slower. This is related to the fact that in the low-temperature phase the nearest singularity is the two-particle cut, so that the convergence radius r_- of the Taylor expansion of $g_-^{-1}(Q)$ is $r_- = 2\sqrt{S_M^-}$, and therefore,

$$c_{n+1}^- \approx -\frac{1}{4 S_M^-} c_n^- \approx -0.27 c_n^- . \tag{15}$$

The large-order coefficients $C_1^\pm, C_2^\pm$, and $C_3^\pm$ have been computed theoretically within the ϵ expansion to order ϵ^3 [24] in the high-temperature phase and to order ϵ^2 in the low-temperature phase [33]. Using the ϵ-expansion results, we obtain

$$C_1^+ \approx 0.92, \qquad C_2^+ \approx 1.8, \qquad C_3^+ \approx -2.7. \tag{16}$$

The corresponding low-temperature parameters C_n^- can be derived from the high-temperature C_n^- by using a set of relations derived in Ref. [28]:

$$\frac{C_1^+}{C_1^-} = U_2^{-1} U_\xi^{2-\eta},$$

$$\frac{C_2^+}{C_2^-} = -U_0 U_\xi^{(1-\alpha)/\nu},$$

$$\frac{C_3^+}{C_3^-} = -U_\xi^{1/\nu}, \tag{17}$$

where

$$U_0 = \frac{A^+}{A^-}, \quad U_2 = \frac{C^+}{C^-}, \quad U_\xi = \frac{f^+}{f^-}. \tag{18}$$

Here, $C^\pm$ and $f^\pm$ are the amplitudes of the susceptibility and of the second-moment correlation length defined above, while $A^\pm$ are defined from the critical behavior of the specific heat, $C_H \approx A^\pm |t|^{-\alpha}$. Using the estimates of Ref. [22] (other estimates can be found in Refs. [3,35–40]), we obtain

$$C_1^- = 1.275(10)\, C_1^+ \approx 1.17,$$

$$C_2^- = -0.728(5)\, C_2^+ \approx -1.3,$$

$$C_3^- = -0.345(2)\, C_3^+ \approx 0.9. \tag{19}$$

The large-momentum behavior of the structure factor has also been studied experimentally and the behavior (7) has been explicitly verified in the high-temperature phase. In particular, the exponent η and the constant C_1^+ have been determined. Reference [10] studied the structure factor for the binary mixture 3-methylpentane–nitroethane. By analyzing the experimental data with Bray's approximation they found $\eta = 0.017(15), C_1^+ = 0.96(4)$, while using two different approximations proposed in Ref. [23] they obtained $\eta = 0.020(17), C_1^+ = 0.95(4)$ and $\eta = 0.030(25), C_1^+ \approx 0.95(4)$. Reference [12] found $\eta = 0.0300(15)$ and $C_1^+ = 0.92(1)$, and Ref. [19] reported $\eta = 0.042(6)$ and $C_1^+ = 0.915(21)$. No unbiased determination of C_2^+ and C_3^+ is available. Fixing $C_2^+ + C_3^+ = -0.9$ (the ϵ-expansion result of Ref. [24]), Ref. [19] obtained $C_2^+ = 2.05(80)$ and $C_3^+ = -2.95(80)$, in reasonable agreement with the ϵ-expansion predictions.

C. Bray's approximation

In order to compare with the experimental data it is important to know the function $g_\pm(Q)$ for all values of Q. For the high-temperature $g_+(Q)$, several interpolations have been proposed with the correct large- and small-Q behavior [6,32,23–25,9]. The most successful one is due to Bray [24], which incorporates the expected singularity structure of $g_+(Q)$. Here, we present Bray's interpolation together with its generalization to the low-temperature phase.

In this approach, one assumes $g_\pm^{-1}(Q)$ to be well defined in the complex Q^2 plane, with a cut on the negative real Q^2 axis, starting at $Q^2 = -r_\pm^2$, where, as discussed above, $r_+^2 = 9 S_M^+, r_-^2 = 4 S_M^-$. Then

$$g_{\pm}^{-1}(Q)=\frac{2\sin\pi\eta/2}{\pi C_1^{\pm}}\int_{r_\pm}^{\infty}du\,u^{1-\eta}F_{\pm}(u)\times\left[\frac{S_M}{u^2-S_M}+\frac{Q^2}{u^2+Q^2}\right],\tag{20}$$

where $F_{\pm}(u)$ is the spectral function, which must satisfy $F_{\pm}(+\infty)=1, F_{\pm}(r_{\pm})=0$, and $F_{\pm}(u)\geqslant 0$ for $u\geqslant r_{\pm}$. Notice the appearance of the constant $C_1^{\pm}$, which is determined, once $F_{\pm}(u)$ is given, by requiring $g_{\pm}^{-1}(0)=1$.

In order to obtain an approximation one must specify $F_{\pm}(u)$. Bray [24] proposed to use a spectral function that gives exactly the Fisher-Langer asymptotic behavior, i.e.,

$$F_{\pm,B}(u)=\frac{P_{\pm}(u)-Q_{\pm}(u)\cot\frac{1}{2}\pi\eta}{P_{\pm}(u)^2+Q_{\pm}(u)^2},\tag{21}$$

where

$$P_{\pm}(u)=1+\frac{C_2^{\pm}}{u^p}\cos\frac{\pi p}{2}+\frac{C_3^{\pm}}{u^{1/\nu}}\cos\frac{\pi}{2\nu},$$

$$Q_{\pm}(u)=\frac{C_2^{\pm}}{u^p}\sin\frac{\pi p}{2}+\frac{C_3^{\pm}}{u^{1/\nu}}\sin\frac{\pi}{2\nu},\tag{22}$$

with $p\equiv(1-\alpha)/\nu$. These definitions do not specify the spectral functions completely since several quantities are still unknown. First of all, we should fix the critical exponents. We will use the estimates of Ref. [22], obtained from the analysis of high-temperature expansions for improved models:

$$\gamma=1.2373(2),\quad \nu=0.63012(16),$$
$$\eta=0.03639(15),\quad \alpha=0.1096(5).\tag{23}$$

Several other determinations are reported in Refs. [30,40–47]. For a comprehensive review see Ref. [3]. For S_M^+ we use the estimate labeled by IHT reported in Table I, while for S_M^- we employ the low-temperature prediction of Ref. [30]; see Table I. We must also fix $C_2^{\pm}$ and $C_3^{\pm}$. In the high-temperature phase, Bray proposes to fix $C_2^+ + C_3^+$ to its ϵ-expansion value $C_2^+ + C_3^+ = -0.9$ and then to determine these constants by requiring $F_{+,B}(r_+)=0$. These conditions completely fix the spectral function and thus the structure factor. As a check, we can compare the estimates of c_n^+ and C_n^+ obtained by using Bray's approximation $g_{+,B}(Q)$ with the previously quoted results. We obtain

$$C_1^+\approx 0.918,\qquad C_2^+\approx 2.56,\qquad C_3^+\approx -3.46,$$
$$c_2^+\approx -4.2\times 10^{-4},\qquad c_3^+\approx 1.0\times 10^{-5}.\tag{24}$$

The constants C_1^+, C_2^+, and C_3^+ are in reasonable agreement with the ϵ-expansion results (16), while c_2^+ and c_3^+ are close to the estimates reported in Table I. Bray's approximation is reported in Fig. 1. Note that the result changes by less than 0.1% for $Q<100$ if η and S_M^+ are varied within one error bar. Also $C_2^+ + C_3^+$ does not play an important role. For instance, by using $C_2^+ + C_3^+ = -0.8$ or -1.0, $g_{+,B}(Q)$ varies by 0.1% at $Q=10$ and 0.5% at $Q=100$.

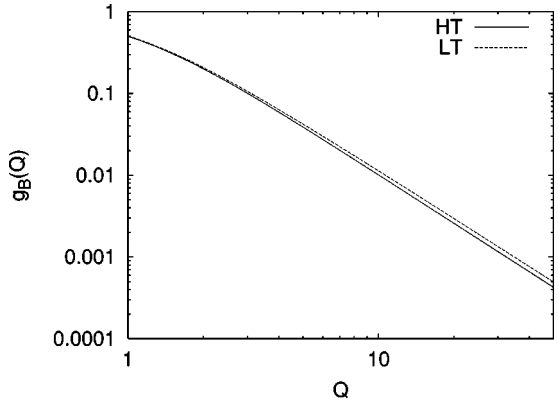

FIG. 1. Scaling functions $g_{\pm}(Q)$ versus Q in Bray's approximation. We report the high- (HT) and low- (LT) temperature scaling functions.

In the low-temperature phase, we have tried to follow again Bray's strategy. We have first set $C_2^- + C_3^- = -0.4$ and required $F_{-,B}(r_-)=0$. However, the resulting estimates of C_n^- and c_n^- are not in agreement with the previous results: we find $C_1^-\approx 0.87, c_2^-\approx -1\times 10^{-3}$. Little changes if we fix $C_2^+ + C_3^+ = -0.9$ and use the relations (17). For this reason, we have given up requiring $F_{-,B}(r_-)=0$ and we have simply set $C_2^- = -1.3, C_3^- = 0.9$, as obtained in the previous section. Then, Bray's approximation gives

$$C_1^-\approx 1.0,\qquad c_2^-\approx -1.1\times 10^{-2},\qquad c_3^-\approx 1.7\times 10^{-3},\tag{25}$$

which are close to previous estimates. A plot of Bray's approximation in the low-temperature phase is also given in Fig. 1. Note that the structure factors in the high- and low-temperature phases are very similar.

III. MONTE CARLO RESULTS

We determine the structure factor in the region of small k—as we shall see, we are able to reach $k\approx 5\text{-}10/\xi$ by means of a large-scale Monte Carlo simulation. We consider the Ising model on a cubic lattice, i.e., the Hamiltonian

$$\mathcal{H}=-\beta\sum_{\langle ij\rangle}\sigma_i\sigma_j,\tag{26}$$

where $\sigma_i=\pm 1$ and the summation is over nearest-neighbor pairs $\langle ij\rangle$. We measure the structure factor

TABLE II. For the three lattices considered, (a), (b), and (c), we report the number of iterations $N_{\rm it}$, the susceptibility χ, the second-moment correlation length ξ, and $h(q;\beta,L)$ for $n=qL/(2\pi)$.

	(a)	(b)	(c)
$N_{\rm it}$	4.35×10^6	3.2×10^6	2.14×10^6
χ	669.9(4)	1501(2)	6339(10)
ξ	13.050(7)	19.739(14)	41.16(5)
n		$h(q;\beta,L)$	
1	−0.0009(9)	−0.0015(11)	−0.0002(17)
2	−0.0002(11)	0.0003(14)	0.0001(25)
3	0.0017(12)	0.0027(16)	0.0019(27)
4	0.0039(13)	0.0065(17)	0.0042(27)
5	0.0063(13)	0.0096(18)	0.0067(28)
6	0.0093(13)	0.0135(18)	0.0095(28)
7	0.0128(13)	0.0179(18)	0.0123(28)
8	0.0178(13)	0.0232(19)	0.0141(28)
9	0.0222(14)	0.0281(18)	0.0179(28)
10	0.0270(13)	0.0335(19)	0.0204(28)
11	0.0326(14)	0.0398(18)	0.0234(29)
12	0.0383(13)	0.0459(17)	0.0263(28)
13	0.0438(13)	0.0521(17)	0.0290(29)
14	0.0510(13)	0.0593(18)	0.0324(29)
15	0.0579(13)	0.0666(18)	0.0353(28)
16	0.0647(14)	0.0736(18)	0.0380(28)
17	0.0722(13)	0.0815(18)	0.0409(29)
18	0.0806(13)	0.0896(18)	0.0437(28)
19	0.0887(14)	0.0986(17)	0.0478(28)
20	0.0975(13)	0.1078(18)	0.0506(29)
21	0.1072(14)	0.1168(18)	0.0538(29)
22	0.1158(14)	0.1271(18)	0.0576(28)
23	0.1258(14)	0.1366(18)	0.0616(28)
24	0.1367(14)	0.1473(18)	0.0642(29)
25	0.1472(14)	0.1583(18)	0.0676(28)

$$S(q;\beta,L)=\frac{1}{3}\sum_{x,y,z}(e^{iqx}+e^{iqy}+e^{iqz})\langle\sigma_{(0,0,0)}\sigma_{(x,y,z)}\rangle \tag{27}$$

for three different values of β and L: (a) $L=128,\beta=0.2204$; (b) $L=128,\beta=0.2210$; (c) $L=256,\beta=0.221\,45$. Of course, in Eq. (27) $q=2\pi n/L$, where n is an integer. In the simulation we used the Swendsen-Wang algorithm, starting from random configurations and discarding $(2-4)\times10^4$ iterations. The results of the simulations are reported in Table II. We report the number of iterations, $N_{\rm it}$, the susceptibility χ, the second-moment correlation length ξ, and $h(q;\beta,L)$,

$$h(q;\beta,L)\equiv\ln\left[\frac{(1+q^2\xi^2)S(q;\beta,L)}{\chi}\right], \tag{28}$$

which directly measures the deviations from a purely Ornstein-Zernike behavior.

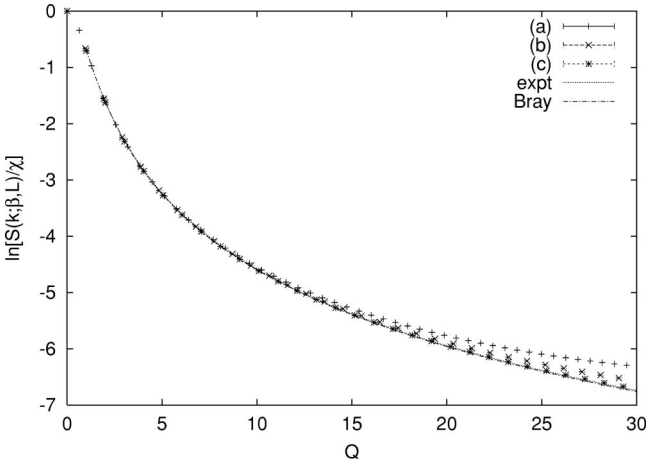

FIG. 2. Function $S(q;\beta,L)/\chi$ versus $Q\equiv q\xi$ for the three cases (a), (b), and (c). We also report the experimental results of Ref. [19], ''expt,'' and Bray's approximation, ''Bray.''

In Fig. 2 we plot $S(q;\beta,L)/\chi$ for the three lattices considered—errors are smaller than the size of the points—together with the experimental results of Ref. [19] for CO_2 and Bray's approximation. We observe good agreement, the numerical data for lattice (c) being close to the experimental ones.

However, at a closer look one observes tiny deviations of order 1%–2%. In order to observe better the differences among the different approximations and data, it is useful to plot the function $h(q;\beta,L)$ which converges to $\ln[(1+Q^2)g_+(Q)]$ in the scaling limit. We have been able to observe accurately [i.e., at the level of one error bar, approximately 0.3% on $g_+(Q)$] this convergence only up to $Q\approx4$, as can be seen in Fig. 3. Indeed, only in this region do we observe a good overlap of the results for the two lattices (b) and (c), which have the largest values of ξ. As a further check, we can compare the numerical results with the small-Q expansion (6) which is expected to converge rapidly up to

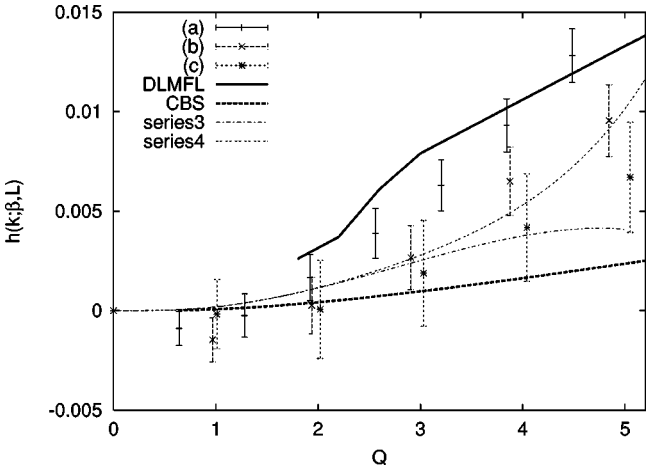

FIG. 3. Function $h(q;\beta,L)$ versus $Q\equiv q\xi$ for the three cases (a), (b), and (c). We also report the experimental results of Ref. [19] (DLMFL) and of Ref. [10] (CBS), and the small-Q approximations ''series3'' and ''series4.''

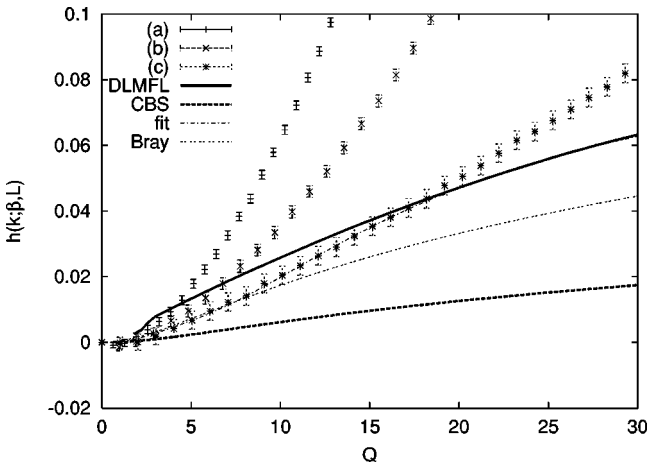

FIG. 4. Function $h(q;\beta,L)$ versus $Q\equiv q\xi$ for the three cases (a), (b), and (c). We also report the experimental results of Ref. [19] (DLMFL) and of Ref. [10] (CBS), a phenomenological interpolation (fit), and Bray's approximation (Bray).

$Q\approx 3$. Using Eq. (6) to order Q^6 (Q^8) we obtain the curve labeled "series3" ("series4") in Fig. 3. The data (c), which correspond to $L=256$, are in perfect agreement, confirming that in this region we are seeing the correct asymptotic behavior. In Fig. 3 we also report [48] the experimental results of Refs. [19,10]. The results of Ref. [19] are systematically higher than the Monte Carlo results, indicating that, at least in this region, the experimental error on the structure factor is approximately of order 0.5%–1%. The results of Ref. [10] are in better agreeement: This is essentially due to the specific interpolation used, which has the correct behavior for $Q\to 0$.

For larger values of Q, we are not able to observe scaling, as can be seen in Fig. 4. According to standard renormalization-group theory,

$$h(q;\beta,L)=h_1(Q,L/\xi)+L^{-\omega}h_2(Q,L/\xi)+\cdots, \quad (29)$$

where [22] $\omega=0.83(5)$. Thus, we could try to extrapolate in L at L/ξ fixed and then take the limit $L/\xi\to\infty$. Lattices (b) and (c) have approximately the same $L/\xi, L/\xi\approx 6$ and thus, in principle, one should be able to extrapolate in L. In practice, corrections increase quickly with Q (see Fig. 4) and no reliable extrapolation can be done. In any case, we believe we can still use the numerical data presented in Fig. 4 to conclude conservatively that, for $Q\lesssim 15$–$20, h(q;\beta,L)$ for lattice (c) is a good approximation to the limiting function with an error at most of 0.02, i.e., that we can use our data (c) to compute $g_+(Q)$ with a 2% precision up to $Q\lesssim$15-20.

In Fig. 4 we also report Bray's approximation. Such an approximation agrees nicely with the Monte Carlo results (c) up to $Q\approx 10$ and, as expected, it is lower in the region $Q\gtrsim 10$ where we expect the results (c) to be higher than the scaling limiting curve. Bray's function looks therefore a reasonable approximation to the universal scaling function. Comparing with experiments, we note that Bray's function is somewhat lower than the experimental data of Ref. [19] by 1%–2%. The older experimental results [48] of Ref. [10] are significantly lower, but it should be noticed that these results are far less accurate than the more recent ones, as can be understood by comparing the errors on the estimates of η presented at the end of Sec. II B.

For the computations of the next section, it is important to have an estimate of the structure factor with a reasonable error bar. For this purpose, we determine a second interpolation that is in better agreement with the experimental data of Ref. [19]. We will obtain an error by comparing the results obtained using this interpolation and Bray's approximation. This interpolation may be obtained by considering expressions that agree with the numerical data for lattice (c) in the region $Q<Q_{\rm max}\approx 15$. We shall use again the spectral representation (20), since such an expression gives automatically the behavior (14) and ensures the correct small-Q behavior. In order to obtain the correct large-Q behavior, we use a generalization of the spectral function proposed by Bray, i.e.,

$$F_{\rm fit}(u)=F_B(u)(1-u^{-2})\left(1+\sum_{n=2}^{n_{\rm max}} a_n u^{-n}\right). \quad (30)$$

Such an expression is purely phenomenological. The first term has been introduced to guarantee that $F_{\rm fit}(1)=0$ as generally expected, while corrections of order $1/u$ have been avoided, since they would give rise to terms of order $1/Q^{2-\eta-1}$ for $Q\to\infty$ that are stronger than those appearing in the Fisher-Langer behavior (7). In Eqs. (20) and (22) we use the ϵ-expansion estimates (16) and the values of the exponents reported in Eq. (23). The constants a_n are fixed by requiring $g_+^{-1}(0)=1$ and $g_+(Q)$ to fit the numerical data (c) up to $Q\leqslant Q_{\rm max}$. If $Q_{\rm max}=15$, a good fit is obtained by taking $n_{\rm max}=6$ and $a_2=-574.128$, $a_3=7588.59$, $a_4=-29\,558.9$, $a_5=43\,740.7$, and $a_6=-21\,715.6$. The corresponding curve labeled "fit" is reported in Fig. 4. The results depend on $Q_{\rm max}$ used in the fit and tend to give a lower curve if smaller values of $Q_{\rm max}$ are used. However, it is interesting to remark that, with the choice $Q_{\rm max}=15$, the interpolation is in excellent agreement with the experimental data for all $Q>15$; see Fig. 4.

Finally, it is interesting to remark that the Ornstein-Zernike approximation differs at most 1% from the correct expression for $Q\lesssim 5$, while for $Q\gtrsim 5$ the Fisher-Langer formula can be applied, as already observed in many experimental works; see, e.g., Refs. [16,18,20,21].

IV. TURBIDITY

The turbidity τ is defined as the attenuation of the transmitted light intensity per unit optical path length due to the scattering with the sample. Explicitly, it is given by

$$\tau\sim\int d\Omega\, S(k)\left[1-\frac{1}{2}\sin^2\theta\right], \quad (31)$$

where $k=2k_0\sin(\theta/2), k_0=2\pi n/\lambda$ is the momentum of the incoming radiation in the medium, λ the corresponding wavelength in vacuum, n the refractive index, and $\Omega=(\phi,\theta)$ the solid angle. By using Eq. (1), in the high-temperature phase we can write the turbidity in the form

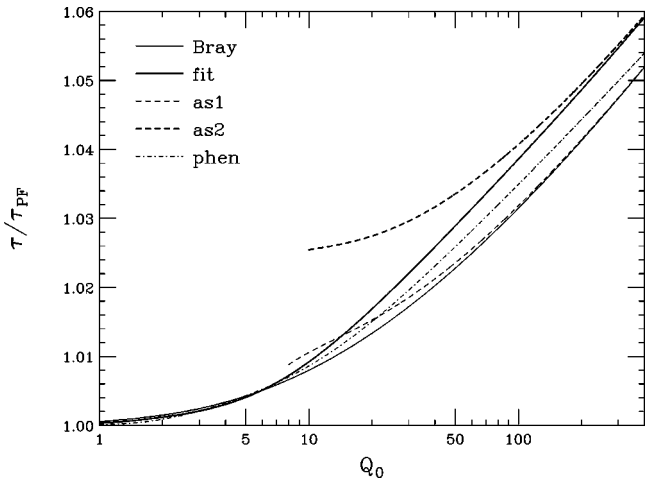

FIG. 5. Ratio $\tau/\tau_{\rm PF}$ versus Q_0 using Bray's approximation, "Bray," and the phenomenological approximation, "fit." We also report the corresponding asymptotic expression $\tau_{\rm as}/\tau_{\rm PF}$ ("as1" and "as2"), where $\tau_{\rm as}$ is defined in Eq. (34), and the phenomenological approximation (36), "phen," valid for $Q_0 \leqslant 100$. In "as1" we use $C_1^+ = 0.917\,97$, $K = 0.128\,735$; in "as2" we use $C_1^+ = 0.92$, $K = 0.160\,734$.

$$\tau = \frac{2\tau_0 t^{-\gamma}}{Q_0^2} \int_0^{2Q_0} Q dQ\, g_+(Q) \left[1 - \frac{Q^2}{2Q_0^2} + \frac{Q^4}{8Q_0^4} \right], \quad (32)$$

where $Q_0 \equiv k_0 \xi$ and τ_0 is a constant that can be assumed temperature independent in a neighborhood of the critical point.

For small values of Q_0, the Ornstein-Zernike approximation can be used obtaining the Puglielli-Ford expression [8]

$$\tau_{\rm PF} = \tau_0 t^{-\gamma} \left[\frac{2a^2 + 2a + 1}{a^3} \ln(2a+1) - \frac{2(a+1)}{a^2} \right], \quad (33)$$

where $a = 2Q_0^2$.

We can also compute the behavior for large Q_0 by using Eq. (7). We obtain

$$\tau_{\rm as} = \frac{2\tau_0 t^{-\gamma}}{Q_0^2} \left[C_1^+ (2Q_0)^\eta \frac{\eta^2 + 2\eta + 8}{\eta(\eta+2)(\eta+4)} - \frac{C_1^+}{\eta} + K + O(Q_0^{\eta - (1-\alpha)/\nu}) \right], \quad (34)$$

where

$$K = \int_0^1 Q dQ g_+(Q) + \int_1^\infty Q dQ [g_+(Q) - C_1^+ Q^{\eta - 2}]. \quad (35)$$

In order to obtain τ for all values of Q_0 we must use a specific form for $g_+(Q)$. We will use here Bray's approximation and the interpolation formula obtained using Eq. (30) with $n_{\rm max}=6, Q_{\rm max}=15$. The difference between the results obtained using these two expressions provides the error on our results. In Fig. 5 we report $\tau/\tau_{\rm PF}$ using the two different approximations together with their asymptotic expression $\tau_{\rm as}/\tau_{\rm PF}$. In Bray's approximation $K = 0.128\,735$ while in the second one $K = 0.160\,734$. The deviations from the Puglielli-Ford behavior are very small and for $Q_0 \gtrsim 100$ are well described by the asymptotic expression (34) with $C_1^+ \approx 0.92$ and $K = 0.145(16)$. Estimates of the turbidity for $1 \lesssim Q_0 \lesssim 100$ can be found in Table III. For $Q \leqslant 100$ one can use the phenomenological formula

$$\tau = \tau_{\rm PF} [0.666421 + 0.242399(1 + 0.0087936 Q_0^2)^{0.018195} + 0.0911801(1 + 0.09 Q_0^4)^{0.0090975}], \quad (36)$$

which is also reported in Fig. 5 ("phen").

We wish finally to compare our results with the approximate expression given by Ferrell [49], which is valid for $Q_0 \gg 1$ and $\eta \ln Q_0 \ll 1$, i.e., for $1 \ll Q_0 \ll e^{1/\eta} \approx 9 \times 10^{11}$. By expanding Eq. (34) and setting $L = \ln(4Q_0^2)$ as in Ref. [49], we obtain

$$\tau \approx \frac{\tau_0 t^{-\gamma}}{Q_0^2} \left[C_1^+ (L-1) + C_1^+ \eta \left(\frac{L^2}{4} - \frac{L}{2} + \frac{3}{4} \right) + K \right]. \quad (37)$$

In order to compare with Ferrell's results, we must compute $\tau/[4\tau_0 t^{-\gamma} g(2Q_0)]$. Since, using the same approximations, $g(2Q_0) = C_1^+ (2Q_0)^{-2} [1 + \eta L/2 + O(\eta^2)]$, we obtain

$$\frac{\tau}{4\tau_0 t^{-\gamma} g(2Q_0)} \approx L - 1 - \frac{\eta L^2}{4} + \eta \left(\frac{3}{4} + \frac{K}{\eta C_1^+} \right). \quad (38)$$

This formula agrees with Ferrell's expression once we recognize that $K = O(\eta)$ since $K = 0$ for a purely Ornstein-Zernike behavior. Numerically, we predict $3/4 + K/(\eta C_1^+) \approx 5.1(5)$, which is smaller than Ferrell's numerical result 8.4. Ferrell's expression predicts a turbidity that is somewhat larger than ours. Indeed, his numerical result implies

TABLE III. Ratio $\tau/\tau_{\rm PF}$. We use here (a) Bray's approximation and (b) a general phenomenological interpolation based on Eq. (30) with $n_{\rm max}=6$ and $Q_{\rm max}=15$.

Q_0	(a)	(b)
5	1.004	1.004
10	1.008	1.009
15	1.011	1.014
20	1.013	1.017
25	1.015	1.020
30	1.017	1.022
35	1.019	1.024
40	1.020	1.026
45	1.022	1.028
50	1.023	1.029
60	1.025	1.031
70	1.027	1.034
80	1.029	1.036
90	1.030	1.037
100	1.032	1.039

$K \approx 0.26$ in Eq. (34), and as consequence we would obtain $\tau/\tau_{\rm PF} \approx 1.06$ [1.085] for $Q_0 = 100$ [1000], to be compared with our prediction $\tau/\tau_{\rm PF} \approx 1.036(4)$ [1.069(3)].

Another expression for the turbidity that takes into account the anomalous decay of the structure factor is given in Ref. [50]. It assumes that [51] $g_+(Q) = (1 + cQ^2)^{-1+\eta/2}$, where $c = 1/(1-\eta/2)$. It follows that

$$\tau = 4\tau_0 t^{-\gamma} \frac{[(2b+1)^{\eta/2} - 1][4 - 2b(\eta - 4) + b^2(\eta^2 + 2\eta + 8)] - 4\eta b(1+b)}{b^3 \eta (2+\eta)(4+\eta)}, \tag{39}$$

where $b = 4Q_0^2/(2-\eta)$. Such an expression, however, predicts a turbidity that is too large. For instance, for $Q_0 = 10$ it gives $\tau/\tau_{\rm PF} \approx 1.05$, to be compared with our prediction $\tau/\tau_{\rm PF} \approx 1.008$; cf. Table III.

Note the correct turbidity τ is larger than $\tau_{\rm PF}$ since $g_+(Q)$ decreases slower for $Q \to \infty$ than the Ornstein-Zernike approximation. However, this is apparently in contrast with the experimental results for the binary fluid mixture methanol-cyclohexane presented in Ref. [52].

ACKNOWLEDGMENTS

The work of V.M.M. was supported by European Commission Contract No. HPMF-CT-2000-00450 and by OCYT (Spain), Project No. FPA2001-1813.

[1] *Phase Transitions, Status of the Experimental and Theoretical Situation, Cargèse 1980*, edited by M. Lévy, J. C. Le Guillou, and J. Zinn-Justin (Plenum, New York, 1981).
[2] M. A. Anisimov, *Critical Phenomena in Liquids and Liquid Crystals* (Gordon and Breach, New York, 1991).
[3] A. Pelissetto and E. Vicari, e-print cond-mat/0012164, Phys. Rep. (to be published).
[4] The structure factor directly determines the scattered light intensity in the absence of multiple scattering. However, multiple scattering is important in experiments on fluids and it is therefore essential to perform the appropriate corrections to the data. See, e.g., Ref. [2] and J.G. Shanks and J.V. Sengers, Phys. Rev. A **38**, 885 (1988); A.E. Bailey and D.S. Cannell, Phys. Rev. E **50**, 4853 (1994); L. Cipelletti, *ibid.* **55**, 7733 (1997). Note also that we consider here only Rayleigh elastic scattering, which is the dominant contribution near the critical point; see, e. g., Ref. [2].
[5] M.E. Fisher, J. Math. Phys. **5**, 944 (1964).
[6] M.E. Fisher and R.J. Burford, Phys. Rev. **156**, 583 (1967).
[7] M.E. Fisher and A. Aharony, Phys. Rev. B **10**, 2818 (1974).
[8] V.G. Puglielli and N.C. Ford, Jr., Phys. Rev. Lett. **25**, 143 (1970).
[9] D. Beysens, A. Bourgou, and P. Calmettes, Phys. Rev. A **26**, 3589 (1982).
[10] R.F. Chang, H. Burstyn, and J.V. Sengers, Phys. Rev. A **19**, 866 (1979).
[11] R. Schneider, L. Belkoura, J. Schelten, D. Woermann, and B. Chu, Phys. Rev. B **22**, 5507 (1980).
[12] P. Damay, F. Leclercq, and P. Chieux, Phys. Rev. B **40**, 4696 (1989).
[13] Y. Izumi, Phys. Rev. A **39**, 5826 (1989).
[14] S. Janssen, D.S. Schwahn, and T. Springer, Phys. Rev. Lett. **68**, 3180 (1992).
[15] H. Sato, N. Kuwahara, and K. Kubota, Phys. Rev. E **53**, 3854 (1996).
[16] M. Lesemann, A. Martín, L. Belkoura, D. Woermann, and E. Hoinkis, Ber. Bunsenges. Phys. Chem. **101**, 228 (1997).
[17] M. Bonetti, C. Bagnuls, and C. Bervillier, J. Chem. Phys. **107**, 550 (1997).
[18] M. Bonetti and P. Calmettes, Rev. Sci. Instrum. **68**, 4163 (1997); Int. J. Thermophys. **19**, 1555 (1998).
[19] P. Damay, F. Leclercq, R. Magli, F. Formisano, and P. Lindner, Phys. Rev. B **58**, 12 038 (1998).
[20] M. Bonetti, G. Romet-Lemonne, P. Calmettes, and M.-C. Belissent-Funel, J. Chem. Phys. **112**, 268 (2000).
[21] M. Bonetti, P. Calmettes, and C. Bervillier, J. Chem. Phys. **115**, 4660 (2001).
[22] M. Campostrini, A. Pelissetto, P. Rossi, and E. Vicari, Phys. Rev. E **65**, 066127 (2002).
[23] R.A. Ferrell and D.J. Scalapino, Phys. Rev. Lett. **34**, 200 (1975).
[24] A.J. Bray, Phys. Rev. B **16**, 1248 (1976).
[25] R.A. Ferrell and J.K. Bhattacharjee, Phys. Rev. Lett. **42**, 1505 (1979).
[26] M.E. Fisher and J.S. Langer, Phys. Rev. Lett. **20**, 665 (1968).
[27] E. Brézin, D. Amit, and J. Zinn-Justin, Phys. Rev. Lett. **32**, 151 (1974).
[28] E. Brézin, J.C. Le Guillou, and J. Zinn-Justin, Phys. Rev. Lett. **32**, 473 (1974).
[29] M. Campostrini, A. Pelissetto, P. Rossi, and E. Vicari, Europhys. Lett. **38**, 577 (1997); Phys. Rev. E **57**, 184 (1998).
[30] M. Campostrini, A. Pelissetto, P. Rossi, and E. Vicari, Phys. Rev. E **60**, 3526 (1999).
[31] V. Agostini, C. Carlino, M. Caselle, and M. Hasenbusch, Nucl. Phys. B **484**, 331 (1997); M. Caselle, M. Hasenbusch, and P. Provero, *ibid.* **556**, 575 (1999).
[32] H.B. Tarko and M.E. Fisher, Phys. Rev. Lett. **31**, 926 (1973); Phys. Rev. B **11**, 1217 (1975).
[33] M. Combescot, M. Droz, and J.M. Kosterlitz, Phys. Rev. B **11**, 4661 (1975).
[34] M.E. Fisher and S.-Y. Zinn, J. Phys. A **31**, L629 (1998).
[35] C. Bagnuls, C. Bervillier, D.I. Meiron, and B.G. Nickel, Phys. Rev. B **35**, 3585 (1987); **65**, 149901(E) (2002).
[36] A.J. Liu and M.E. Fisher, Physica A **156**, 35 (1989).

[37] M. Caselle and M. Hasenbusch, J. Phys. A **30**, 4963 (1997).
[38] M. Hasenbusch and K. Pinn, J. Phys. A **31**, 6157 (1998).
[39] S.A. Larin, M. Mönnigmann, M. Strösser, and V. Dohm, Phys. Rev. B **58**, 3394 (1998).
[40] R. Guida and J. Zinn-Justin, J. Phys. A **31**, 8103 (1998).
[41] P. Butera and M. Comi, Phys. Rev. B **65**, 144431 (2002).
[42] B.G. Nickel and J.J. Rehr, J. Stat. Phys. **61**, 1 (1990).
[43] M. Hasenbusch, Int. J. Mod. Phys. C **12**, 911 (2001).
[44] H.W.J. Blöte, L.N. Shchur, and A.L. Talapov, Int. J. Mod. Phys. C **10**, 1137 (1999).
[45] H.G. Ballesteros, L.A. Fernández, V. Martín-Mayor, A. Muñoz Sudupe, G. Parisi, and J.J. Ruiz-Lorenzo, J. Phys. A **32**, 1 (1999).
[46] H.W.J. Blöte, E. Luijten, and J.R. Heringa, J. Phys. A **28**, 6289 (1995).
[47] For the exponent η, which is the relevant quantity for the structure factor, we report here the best estimates [when only γ and ν are reported we computed η using the scaling relation $\gamma=\nu(2-\eta)$] obtained using high-temperature series extrapolations, Monte Carlo simulations, and field-theory computations: $\eta=0.0360(8)$ (Ref. [41]), $\eta=0.0359(7)$ (Ref. [42]), $\eta=0.0362(8)$ (Ref. [43]), $\eta=0.0372(10)$ (Ref. [44]), $\eta=0.0374(12)$ (Ref. [45]), and $\eta=0.0335(25)$ (Ref. [40]). All results are in good agreement with the more precise estimate of Ref. [22] quoted in the text.
[48] In the figures we report an interpolation of the experimental data of Ref. [10]. We use $g_+(Q)=1+Q^2(1+Q^2/9)^{-\eta/2}[1+\eta s(Q)]$, where $s(Q)$ is given in Table II of Ref. [10] and $\eta=0.017$. As can be seen from Fig. 6 in Ref. [10], this expression interpolates the experimental data in the range $0.18<Q<25$ with an error of approximately 1%.
[49] R.A. Ferrell, Physica A **177**, 201 (1991).
[50] P. Calmettes, I. Laguës, and C. Laj, Phys. Rev. Lett. **28**, 478 (1972).
[51] In Ref. [50], the scaling function $g_+(Q)$ is written as $g_+(Q)=1/(1+q^2\xi^2)^{1-\eta/2}$, so that the correlation length defined there does not coincide with the usual second-moment one. In order to be consistent with our normalizations, we have introduced the correction factor c.
[52] D.T. Jacobs, S.M.Y. Lau, A. Mukherjee, and C.A. Williams, Int. J. Thermophys. **20**, 877 (1999).